Analysis of Water Hammering in a Pipe Having an Accumulator

Yong Kweon Suh*

Key words: Accumulator, Water hammering, Throttle resistance, Method of characteristics

Abstract

This paper addresses characteristics of compressible flow dynamics inside a pipe with an accumulator and an inlet orifice. It also presents a simple but stable numerical method associated with the accumulator-orifice calculation. In particular, a focus is given to developing a method of finding an optimum design of the accumulator-orifice system (i.e., the accumulator size and the throttle resistance) that gives the most effective dissipation of the water-hammering problem. It is found that there exists indeed an optimum set of parameter values for the most effective dissipation of the wave energy.

Nomenclature

a : sound velocity, $\sqrt{\beta/\rho}$ [m/s]
A_o : sectional area of the valve throttle (at arbitrary time) [m^2]
A_{oo} : sectional area of the valve throttle (at initial time) [m^2]
A_p : sectional area of the pipe [m^2]
C : characteristic value, inlet of the accumulator (Fig. 2)
C_1, C_2 : arbitrary constants
c_v : velocity coefficient of the valve
D : inner diameter of the pipe [m]
E : arbitrary constant
f : friction coefficient of the pipe
g : gravitational acceleration [m/s^2]
H_R : water depth at the inlet of the pipe [m]
I : number of grids in the x-space
K_{ac}, K_v, K_{v0} : arbitrary constants
L_p : pipe length [m]
L_{ac} : length of the pipe connecting the accumulator [m]
m, n : constants
p : pressure [Pa]
p_{av} : spatio-temporal average of $|1-p/p_\infty|$ (equation (17b))
p_{av0} : p_{av} when accumulator is absent
p_{end} : pressure at the pipe outlet (upstream of the valve) [Pa]
p_∞ : pressure at the quiescent state [Pa]
t : time [s]
t_c : valve-closing time [s]
t_e : final time of computation [s]

* Department of Mechanical Engineering, Dong-A University, Pusan 604-714, Korea

u : flow velocity [m/s]
u_{0s} : flow velocity at the initial steady state [m/s]
u_{av} : spatio-temporal average of $|u/u_{0s}|$ (equation (17a))
u_{av0} : u_{av} when accumulator is absent
u_{in} : u at the inlet of the pipe [m/s]
x : spatial coordinate along the downstream direction [m]
V : volume [m^3]

Greek symbols

β : modulus of the fluid elasticity [Pa]
ζ : head loss coefficient of the throttle for the accumulator
ρ : fluid density [kg/m^3]
τ : relative opening of the valve (equation (16))
δt : time step for the accumulator computation [s]
Δt : time step for the pipe computation [s]
Δx : grid space [m]

Subscripts

1, 2, 3 : indicate positions at the upstream, downstream, and toward the accumulator
ac : accumulator
$ac0$: initial state of the gas in the accumulator
i, N, W : grid points in the space-time space

1. Introduction

Fluid flows inside a duct present a serious problem called water hammering. It occurs when the flow is suddenly blocked by e.g. a valve accompanying a pressure wave. The strength and velocity of the pressure wave is a function of the valve-closing time, the fluid compressibility, elasticity of the duct, and dynamic characteristics of facilities attached to the duct. It is uttermost important to avoid the water hammering in designing a duct system because, when the water hammering occurs, the duct system not only generates noise but also causes fatigue failure or malfunction of attached facilities.

Yum et al.[1] studied, numerically and experimentally, on the separation of fluid column caused by water hammering. Kang et al.[2] analysed performance of a piping system having an air chamber and its effect on the water hammering. Han et al.[3] conducted an experimental study on the water-hammering problem occurring in architectural piping systems by using a 10 m high water tank and a 32 m long pipe. Lee and Kim[4] reported the numerical results on the relationship between the water hammering and the pipe vibration.

In this paper we focus on a pipe system having an accumulator designated to reduce the water hammering. Since the accumulator is connected to the pipe in parallel, it does not affect the fluid flow at steady state. When the water hammering occurs, however, the pressure in the pipe locally fluctuates due to the propagation of the pressure wave. When the local pressure at the junctional point of the accumulator and the pipe is higher than the time average, the fluid flows from the accumulator into the pipe and thus increase of the line pressure is resisted. On the contrary, when the local pressure is lower than the time average, the fluid-flow direction is reversed and thus decrease of the line pressure is similarly compensated. On the other hand, conservation of energy dictates that without a damping mechanism the wave energy is not dissipated. The accumulator is indeed supposed to reduce the abrupt increase or decrease of the line pressure but not as a damper. Therefore if the natural damping effect given by e.g. the

pipe friction is not sufficient enough, additional dampers such as a throttle must be built in an appropriate place. The key engineering issue in this case is selecting the optimum size of the accumulator and the optimum throttle resistance.

The optimization problem raised in the above necessitates the numerical analysis, usually one-dimensional, of the compressible flow inside the pipe. Among others, the method of characteristics (e.g. Wylie and Streeter[5]) is the most frequently used as the numerical method. On the other hand, the pipe friction is simply modelled by a friction law such as the Darcy's law. To account for the dynamical behaviour of the flows, more rigorous laws allow the friction coefficient as a function of the frequency of the flow oscillation as proposed by Zielke,[6] Trikha,[7] Suzuki et al.,[8] and Schohl,[9] but in this study we simply take the friction coefficient as a constant.

The numerical method for the pipe system with accumulators is given by Wylie and Streeter,[5] but it is an iterative method and sometimes requires a very small time step. In this study, a more convenient method is proposed. This paper also addresses the main reason why the conventional method requires a small time step.

The numerical method is then applied to a specific water-hammering problem, where one seeks an optimum accumulator size and an optimum orifice size.

2. Numerical method

For the compressible fluid flowing in a straight pipe, the one-dimensional governing equations are

$$\frac{\partial p}{\partial t}+\beta\frac{\partial u}{\partial x}+u\frac{\partial p}{\partial x}=0 \tag{1}$$

$$\frac{\partial u}{\partial t}+\frac{1}{\rho}\frac{\partial p}{\partial x}+u\frac{\partial u}{\partial x}+\frac{fu|u|}{2D}=0 \tag{2}$$

The method of characteristics is employed here to solve the above set of equations. Since the method is well described in the text of Wylie and Streeter,[5] only a brief description will be given here. Multiplying the constants $\pm a/\beta$ to equation (2) and add the result to (1) yields

$$\frac{du}{dt}\pm\frac{a}{\beta}\frac{dp}{dt}+\frac{fu|u|}{2D}=0 \tag{3}$$

$$\frac{dx}{dt}=\pm a+u \tag{4}$$

where the total derivative d/dt is defined as

$$\frac{d}{dt}=\frac{\partial}{\partial t}+\frac{dx}{dt}\frac{\partial}{\partial x}$$

To discretize equation (3), the x-space is divided into $(I-1)$ segments, and we take the variables u and p defined only at the grid points as unknown. The time step is denoted as Δt, and we take the present time as $t=0$ and the future time as $t=\Delta t$ for convenience (Fig. 1). Applying the Euler's method and discretizing equation (3) gives the following.

$$u_N+\frac{a}{\beta}p_N=C_W\equiv u_W+\frac{a}{\beta}p_W-\frac{fu_W|u_W|}{2D}\Delta t \tag{5}$$

$$u_N-\frac{a}{\beta}p_N=C_E\equiv u_E-\frac{a}{\beta}p_E-\frac{fu_E|u_E|}{2D}\Delta t \tag{6}$$

Here the subscripts designate both the spatial and temporal grid points (Fig. 1), and the con-

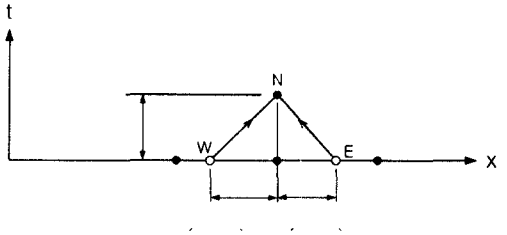

Fig. 1 Schematic illustration of implication given by the equations (3) and (4).

stants C_W and C_E are evaluated by using the temporally known variables. Solving equations (5) and (6) for u_N and p_N provides

$$u_N = \frac{1}{2}(C_W + C_E)$$
$$p_N = \frac{\beta}{2a}(C_W - C_E) \tag{7}$$

Resultantly equation (4) is used in obtaining variables at the two points W and E. However since the two points in general do not coincide with the grid points $i-1$ and $i+1$, respectively, evaluation of C_W and C_E necessitates the interpolation. When the points exactly coincide with the grid points, then the numerical results are the most accurate; however, this happens only for the special case $u=0$. It is also well known that if either of the two points situate outside of the space between $i-1$ and $i+1$ the numerical instability occurs.[5] In view of these points we take the time step Δt as follows.

$$\Delta t = \frac{\Delta x}{a + |u|_{\max}}$$

so that the numerical method becomes both stable accurate.

Setting the boundary conditions for the discrete equation (7) will be addressed in the next section where the method is applied to the actual case.

3. Flow in the pipe with an accumulator

Fig. 2 describes a pipe system containing an accumulator to be numerically solved. As the boundary condition at the upstream end, the pressure there is given by the static pressure, which is constant:

$$p_N = \rho g H_R$$

The flow velocity u_N at the boundary can be obtained from equation (6).

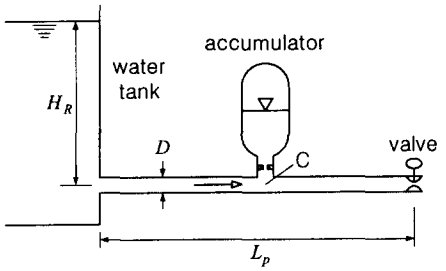

Fig. 2 A water pipe, attached to a tank, with an accumulator and a valve.

To set the boundary conditions at the downstream end, we use the relationship between the velocity and the pressure drop across the valve. Let the pressure in front of the valve p_N, and we can write the formula for u_N the velocity at the point as follows.

$$u_N = K_v\sqrt{p_N}\,, \quad K_v = \frac{A_o c_v}{A_p}\sqrt{\frac{2}{\rho}} \tag{8}$$

where the pressure downstream of the valve is set as 0, i.e. the atmospheric pressure. Combining this and equation (5), we obtain the formula for p_N as

$$p_N = 2\left(\frac{a}{\beta}\right)^2\left[\left(K_v^2 + \frac{2aC_W}{\beta}\right) - \sqrt{\left(K_v^2 + \frac{2aC_W}{\beta}\right)^2 - 4\left(\frac{a}{\beta}\right)^2 C_W^2}\,\right] \tag{9}$$

The velocity in front of the valve is then given by substituting the result into (5).

To obtain boundary conditions at the point where the accumulator is connected (i.e. point C in Fig. 2), we write the relevant equations as follows.

$$u_3 = u_1 - u_2 \tag{10}$$

$$p_{ac} V_{ac}^n = K_{ac} \equiv p_{ac0} V_{ac0}^n \tag{11}$$

$$\rho L_{ac}\frac{du_3}{dt} = p_N - p_{ac} - \frac{1}{2}\zeta\rho u_3|u_3| \tag{12}$$

$$\frac{dV_{ac}}{dt} = -A_p u_3 \tag{13}$$

Equation (10) corresponds to the continuity equation for the space surrounding the point C. Here, the diameter of the connecting pipe is assumed to be the same as that of the main pipe. Equation (11) represents the compression/expansion process of the gas in the accumulator. The exponent n varies usually $1 \sim 1.4$. Equation (12) comes from the momentum principle for the fluid in the connecting pipe, the left-hand side representing the inertial effect of the fluid. Here, L_{ac} denotes the length of the connecting pipe and p_N the pressure at the point C. Further, p_{ac} is the pressure downstream of the throttle, being assumed to be the same as the gas pressure. Equation (13) represents the change of the gas volume in the accumulator caused by inflow/outflow of the fluid through the connecting pipe. On the other hand, in the main pipe, equation (5) applies upstream of the point C (here u_N becomes u_1), and equation (6) applies downstream of C (here u_N becomes u_2). Subtracting one from the other and applying equation (10) provides

$$u_3 = C_W - C_E - \frac{2a}{\beta} p_N \tag{14}$$

Thus four equations (11)~(14) determine four unknowns p_N, u_3, p_{ac} and V_{ac}. The time derivative d/dt used in equations (12) and (13) is of course different from that used in (3) and (4). The former indicates simply a time derivative at a fixed spatial point. We can eliminate p_{ac} and p_N in (12) by using the equations (11) and (14) to obtain

$$\rho L_{ac} \frac{du_3}{dt} = -\frac{K_{ac}}{V_{ac}^n} + \frac{\beta}{2a}(C_W - C_E - u_3) - \frac{1}{2}\zeta \rho u_3 |u_3| \tag{15}$$

Now the governing equations are simply (13) and (15), and the number of unknowns are also reduced to two. Wylie and Streeter[5] propose to neglect L_{ac} making the left-hand side of (15) zero, discretize (13) by the Crank-Nicolson method and finally solve the combined nonlinear equation by using an iterative method.

In order to develop a simpler numerical algorithm, the explicit Euler method has been applied to the equations (13) and (15) without neglecting L_{ac}. In this case the time step δt must be taken smaller than the time step Δt for the main pipe calculation. In another words, when the main-pipe computation for one time step is completed thus supplying the constants C_W and C_E, one must integrate equations (13) and (15) for the interval $t \sim t + \Delta t$ with the time step $\delta t = \Delta t / m$ for an integer m. It has been found from the numerical experiments that as L_{ac} becomes smaller m must be increased due to the numerical instability.

The primary reason why m must be large for small L_{ac} (thus requiring a longer computer time) can be clarified from the analysis to the equations (15) and (13). If, for a sufficiently small value of L_{ac}, the initial condition is applied such that the right-hand side of (15) is not zero, u_3 undergoes a rapid change from the start to make the right-hand side zero. In this case the time scale is proportional to L_{ac}. Therefore due to this rapid behavior the time step δt must be taken small for the numerical stability. On the other hand, during this process the change of V_{ac} is very small, because as seen from equation (13) the change of V_{ac} is caused by the integration of u_3 for such a very short time-interval. After the initial abrupt change of u_3, the right-hand side of (15) becomes almost 0, and V_{ac} (and thus u_3) slowly changes by the equation (13).

Assuming that the initial rapid change of u_3 of the fluid in the main pipe is negligibly effective on the dynamical features and the numerical stability of the main pipe, we propose a new algorithm for the special case of $L_{ac}=0$ as follows. First u_3 is decided from the requirement that the right-hand side of (15) be zero; we simply use the well known formula for finding the roots of the quadratic equation. Then this result is substituted into (13) to obtain a new V_{ac}. Here, V_{ac} in equation (15) is assumed to be known (The validity of the assumption is illustrated previously). It has been found that for $L_{ac}=0$ even $m=1$ gives stable solutions. Otherwise one fails to obtain stable solutions if one follows a procedure in which, for instance, firstly p_{ac} is given from (11) with the initial values of V_{ac} and p_N fixed, secondly u_3 from (12) with the right-hand side set zero, and finally V_{ac} and p_N from (13) and (14).

The water hammering occurs when the valve at the end of the pipe is suddenly closed. The strength of the water hammering depends on the closing time. In this study $A_o(t)$ the sectional area of the valve throttle varies in time as follows (Wylie and Streeter[5]).

$$A_o = A_{oo}\tau(t), \quad \tau(t) = (1 - t/t_c)^E \qquad (16)$$

For $t > t_c$, we set $\tau = 0$.

We need intial values of the flow velocity and pressure. The initial conditions are given from the steady state where the fluid steadily flows and the pressure is not changed at any place within the pipe. At the steady state, the pressure distribution is given by setting the terms $\partial/\partial t$ zero in (1) and (2), eliminating $\partial u/\partial x$ from both equations, and assuming $|u| \ll |a|$ and $u \cong$ const. The velocity is given by substituting the pressure at $x = L_p$ into equation (8). The results are

$$p_{\text{end}} = \frac{\rho g H_R}{1 + f\rho L_p K_{v0}^2/2D}$$

$$u = K_{v0}\sqrt{p_{\text{end}}} \equiv u_{0s}$$

$$p = \rho g H_R - \frac{f\rho u^2}{2D}x$$

where, the constant K_{v0} corresponds to the value of K_v at the instant when the valve starts to open.

4. Numerical results and discussions

First of all, to check the validity of the numerical algorithm, the code is applied to the model problem set by Wylie and Streeter[5]; $a=1200$ m, $\rho=1000$ kg/m^3, $D=0.5$ m, $H_R=150$ m, $L_p=600$ m, $f=0.018$, $E=1.5$, $A_{\infty}c_v=0.009$ m^2, $t_c=2.1$ s. For this model case we set $I=51$ and $m=1$ (all the following results are obtained with $m=1$). In this paper the SI unit is employed. Fig. 3 shows the temporal change of u_{in} and p_{end} obtained from the present code and given by Wylie and Streeter[5] (symbols). It reveals that the two results completely coincide with each other. In this case the nonlinear terms, except the friction term, in (1) and (2)

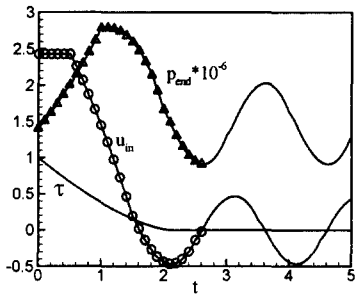

Fig. 3 Numerical results of u_{in}, the inlet velocity, and p_{end}, the pressure at the pipe end, obtained for the case without the accumulator. Symbols indicate the data given by Wylie and Streeter.[5]

are neglected; but including those terms in the calculations gives no appreciable difference. All the numerical results presented in the following are obtained with the nonlinear terms included. The numerical results are also almost invariant even if I is increased to 201.

The most significant parameters associated with the control of the water hammering for the case without the accumulator are the pipe length L_p and the valve-closing time t_c; the pipe diameter is set constant because it plays as a reference length. Fig. 4 shows the dynamical behavior of u_{in} and p_{end} for the case without the accumulator upon variation of the two parameters. For the pipe length 600 m set constant, the smaller t_c results in a larger wave energy, Figs. 4 (a) and (b). Therefore to reduce the water hammering effect, the valve must be closed slowly. However the valve-closing time and the water hammering are related to the pipe length. Figs. 4 (c) and (d) show the numerical results for the case the pipe length being increased four times but the valve-closing times unchanged. It is seen that no appreciable difference exists between large and small t_c. In fact it is effective when t_c is set larger than 4 s. These results also confirm the well known linear theory that the period of wave of the water hammering is proportional to the pipe length.

We now turn to the case with the accumulator. The gas in the accumulator is assumed to undergo an isothermal process so that the constant n is simply set 1. If the accumulator is attached to the pipe line the water hammering can be significantly reduced. To quantify such effect we define a spatio-temporal average of variables after the valve is closed as follows.

$$u_{av} = \frac{1}{L_p(t_e - t_c)} \int_{t_c}^{t_e} \int_0^{L_p} \left| \frac{u}{u_{0s}} \right| dx\,dt \quad (17a)$$

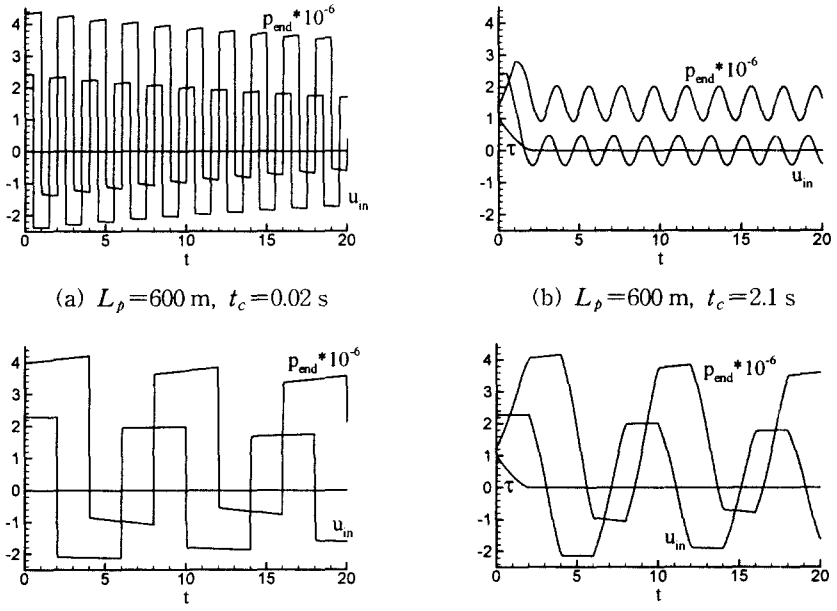

(a) L_p=600 m, t_c=0.02 s (b) L_p=600 m, t_c=2.1 s

(c) L_p=2400 m, t_c=0.02 s (d) L_p=2400 m, t_c=2.1 s

Fig. 4 Transient behavior of u_{in} and p_{end} for different sets of L_p and t_c for the case without the accumulator.

$$p_{av}=\frac{1}{L_p(t_e-t_c)}\int_{t_c}^{t_e}\int_0^{L_p}\left|1-\frac{p}{p_\infty}\right|dxdt \quad (17b)$$

where t_e=50 s. In the mean time, as discussed previously, the strength of the compressive wave depends on the pipe length and the valve-closing time, aside from the accumulator and the inlet orifice size. Therefore to appreciate the pure existence of the accumulator we introduce the ratios u_{av}/u_{av0} and p_{av}/p_{av0}, where u_{av0} and p_{av0} are values of u_{av} and p_{av} given from equations (17a) and (17b) for the case without the accumulator. These quantities thus represent the relative strength of the compressive wave for the case with accumulator based on the case without the accumulator. Hereinafter u_{av}/u_{av0} is called 'relative magnitude of the velocity fluctuation' and p_{av}/p_{av0} 'relative magnitude of the pressure fluctuation'.

Fig. 5 shows contour plots of $\log(u_{av}/u_{av0})$ in the parameter space ($\log V_{ac}$, $\log\zeta$) for 4 pipe lengths. All the parameter values except V_{ac}, ζ and L_p are as given at the beginning of this section, and the number of the grid points I increases from 101 with increase of L_p. The accumulator is situated at the mid point of the pipe. We can see from this figure that there exists a parameter set which gives the least magnitude of $\log(u_{av}/u_{av0})$. Shown in Table 1 are the values of V_{ac} and ζ which pro-

Table 1 Optimum values of V_{ac} and ζ resulting in minimum of u_{av}/u_{av0} for D=0.5 m; also shown are values of p_{av}/p_{av0} at the corresponding parameter set.

L_p [m]	300	600	1200	2400
V_{ac} [m^3]	2.5	3.5	5.6	11
ζ	70000	16000	3200	1000
u_{av}/u_{av0}	1.4%	2.4%	4.0%	8.7%
p_{av}/p_{av0}	0.9%	1.5%	3.7%	8.9%

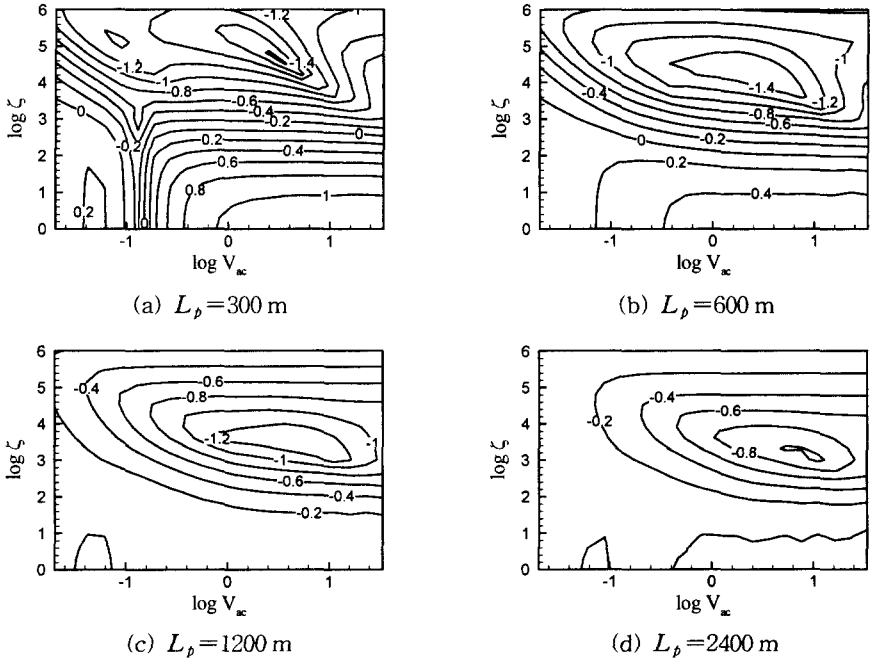

(a) L_p=300 m (b) L_p=600 m

(c) L_p=1200 m (d) L_p=2400 m

Fig. 5 Contour plots of $\log(u_{av}/u_{av0})$ in the parameter space ($\log V_{ac}$, $\log\zeta$) for 4 pipe lengths.

vide the least magnitude of $\log(u_{av}/u_{av0})$ and the corresponding value of u_{av}/u_{av0} in %. It is seen that the presence of the accumulator reduces the relative magnitude of the velocity fluctuation up to 1.4~8.7% of that without the accumulator.

The optimum values of V_{ac} and ζ should be determined of course by considering the relative magnitude of the pressure fluctuation. Fig. 6 shows contour plots of $\log(p_{av}/p_{av0})$ in the parameter space ($\log V_{ac}$, $\log\zeta$) for 4 pipe lengths. Except for the case L_p=300 m, the relative magnitude of the pressure fluctuation consistently decreases as V_{ac} is increased. The numerical values of p_{av}/p_{av0} shown in Table 1 are the corresponding ones when u_{av}/u_{av0} is minimum.

We now discuss the effect of the throttle resistance ζ in a physical view point. When ζ is 0, the magnitude of the velocity and pressure fluctuation cannot be reduced because it corresponds to the case without a damper. It is attributed to this reason that in Figs. 5 and 6, when ζ is below a certain value, the fluctuation increases as ζ decreases. On the other hand, when ζ is too large, it corresponds to the case without an accumulator, and thus one cannot expect the damping effect.

Next, discussion is given to the effect of V_{ac} which represents the accumulator size. It is clear that as V_{ac} tends to 0, it approaches to the case without an accumulator. It is attributed to this reason that in Figs. 5 and 6, except for L_p=300 m, the fluctuation increases as V_{ac} is decreased. When V_{ac} is too large, p_{ac} remains almost constant and the accumulator plays a role as a source/sink of fluid when the line pressure is below/above p_{ac}. Then one may judge that it can reduce the pressure fluctuation. However the velocity fluctuation cannot be decreased. The initial pressure in the accu-

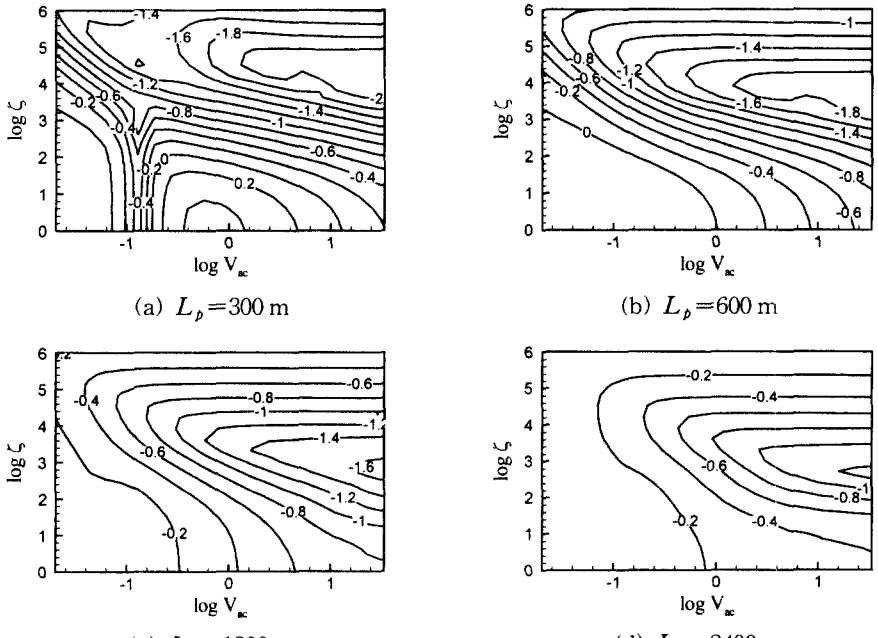

(a) L_p=300 m (b) L_p=600 m

(c) L_p=1200 m (d) L_p=2400 m

Fig. 6 Contour plots of $\log(p_{av}/p_{av0})$ in the parameter space ($\log V_{ac}$, $\log\zeta$) for 4 pipe lengths.

mulator is the same as that at the point C in Fig. 2. After the valve is closed the pressure at C becomes larger than the initial value. On the contrary, the pressure in the accumulator remains almost constant and keeps its initial value since the gas volume is large. Then the fluid in the reservoir flows into the accumulator through the main and connecting pipes almost steadily. It is attributed to this fact that in Fig. 6 the pressure fluctuation decreases as V_{ac} is increased whereas in Fig. 5 the velocity fluctuation does not follow the same trend.

Fig. 7 shows the effect of various sets of parameter values of the accumulator on the transient behavior of u_{in} and p_{end} for L_p=600 m; (a) is for the case without the accumulator, (b) for the case when V_{ac} and ζ are selected as optimum values, (c) for the case when V_{ac} is set very large, and (d) for the case when ζ is set small. In (b) the fluctuations almost completely disappeared at t=4 s. For a large V_{ac}, Fig. 7 (c), the pressure becomes very soon constant, but u_{in} remains a positive value. The reason is attributed to the fact as explained previously.

When the value of V_{ac} is slightly decreased, u_{in} fluctuates significantly around 0, and this is due to the effect of the fluid inertia in the pipe upstream of the accumulator. When V_{ac} is set as optimum and ζ is set small enough, Fig. 7 (d), the magnitude and the period of the u_{in} fluctuation in particular increase. The pressure fluctuation however is not so large. This circumstance is similar to the case in which the elasticity of the pipe material is relatively small; that is, the existence of the accumulator containing a gas provides flexibility to the pipe

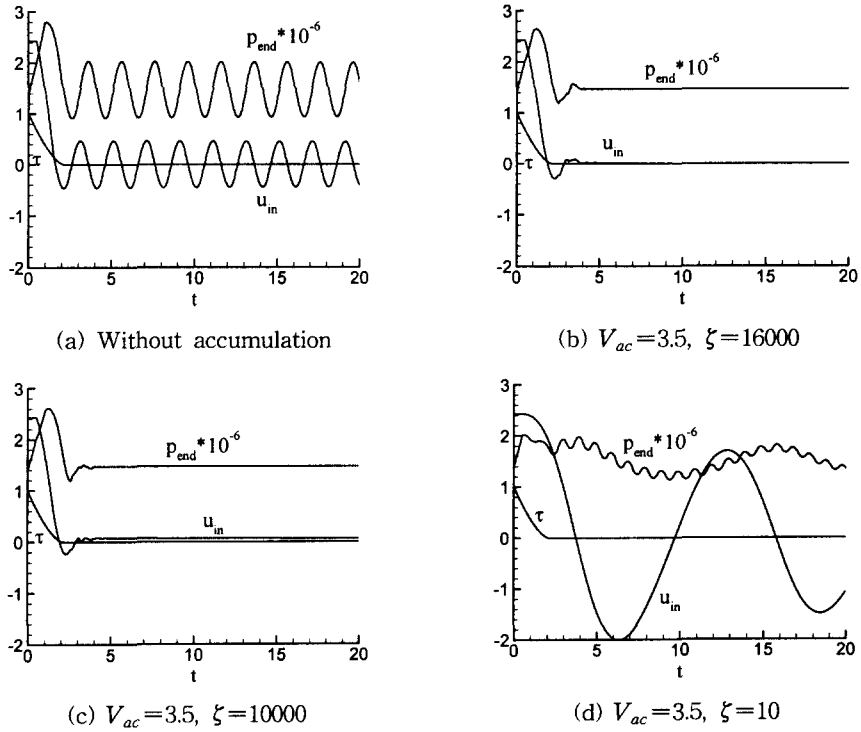

(a) Without accumulation

(b) V_{ac}=3.5, ζ=16000

(c) V_{ac}=3.5, ζ=10000

(d) V_{ac}=3.5, ζ=10

Fig. 7 Effect of various sets of parameter values of the accumulator on the transient behavior of u_{in} and p_{end}.

system on the whole and the direct connection of the accumulator, i.e. lower ζ value, augments such effect. Therefore use of a inlet orifice with a suitable resistance is mandatory for optimum control of the water hammering.

To confirm such similarity, the case with lower sound velocity (i.e. softer pipe material) without the accumulator is numerically solved at L_p=600 m, t_c=2.1 s and a=200 m/s. Fig. 8 shows the results. It is seen that in overall the amplitude and period of the velocity and pressure fluctuations are in the same order as those of Fig. 7 (d).

Turning our attention to Table 1, we can see that as the pipe is longer the accumulator as a damper is less effective. This table also provides the optimum accumulator size for a given parameter set. Further it indicates that as the pipe is longer the optimum size of the accumulator becomes larger and the optimum throttle resistance is smaller.

In addition, it must be stressed that the present results are obtained only for the pipe inner diameter D=0.5 m. For a smaller pipe diameter it may be intuitively conjectured that an optimum size of the accumulator should be smaller, but this must be confirmed from numerical works for smaller diameters, which is remained as future study. Applying a frequency-dependent friction coefficient to the water hammering problem is also an interesting topic.

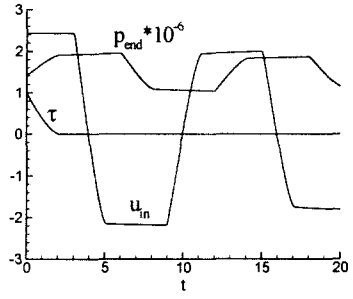

Fig. 8 Numerical result for a=200 m/s for the case without the accumulator at L_p= 600 m.

5. Conclusions

Proposed in this study is a simple explicit Euler method which can resolve the dynamical behavior of flows inside a pipe accompanying a water hammering phenomenon. This study also clarified the relevant reason for the proposed method.

The proposed method is then applied to the water hammering problem of a 0.5 m-diameter pipe system. It is shown that an optimum set of accumulator size and the inlet-orifice resistance exist, which is the most effective in damping the compressive wave.

The numerical method proposed in this study can be applied to various engineering areas, which use pipe systems to transport fluids, namely power plants, urban water supply, and fluid powers.

References

1. Yum, M. O., Lee, J. K., Lee, I. Y. and Kim, H. K., 1988, A study on fluid transient accompanying column separation in oil hydraulic pipeline, Trans. KSME, Vol. 12, No. 5, pp. 984-991.
2. Kang, S. H., Ryu, H. S. and Park, M. S., 1992, Design and performance prediction of an air chamber for reduction of water hammering, Korean Journal of Air-Conditioning and Refrigeration Engineering, Vol. 4, No. 1, pp. 57-64.
3. Han, H. T., Kim, J. M. and Kim, J. P., 1994, A study on water hammer phenomena in piping systems of buildings, Trans. KSME, Vol. 18, No. 9, pp. 2251-2256.
4. Lee, U. and Kim, J. H., 1995, Internal flow-induced vibration of a series pipeline, Trans. KSME, Vol. 19, No. 12, pp. 3230-3240.
5. Wylie, E. B. and Streeter, V. L., 1982, Fluid transients, FEB Press.
6. Zielke, W., 1968, Frequency-dependent friction in transient pipe flow, ASME J. Basic

Engineering, Vol. 90, pp. 109-115

7. Trikha, A. K., 1975, An efficient method for simulating frequency-dependent friction in transient liquid flow, ASME J. Fluids Engineering, Vol. 97, pp. 97-105.
8. Suzuki, K., Taketomi, T. and Sato, S., 1991, Improving Zielke's method of simulating frequency-dependent friction in laminar liquid pipe flow, ASME J. Fluids Engineering, Vol. 113, pp. 569-573.
9. Schohl, G. A., 1993, Improved approximate method for simulating frequency-dependent friction in transient laminar flow, ASME J. Fluids Engineering, Vol. 115, pp. 420-424.